HHS Public Access

Author manuscript

Neuropharmacology. Author manuscript; available in PMC 2016 August 01.

Published in final edited form as:

Neuropharmacology. 2015 August ; 95: 405–414. doi:10.1016/j.neuropharm.2015.04.016.

Activation of α7 nicotinic acetylcholine receptors increases intracellular cAMP levels via activation of AC1 in hippocampal neurons

Qing Cheng and **Jerrel L. Yakel**

Neurobiology Laboratory, NIEHS / NIH, 111 T.W. Alexander Dr., Durham, NC 27709

Abstract

The activation of α7 nAChRs has been shown to improve hippocampal-dependent learning and memory. However, the molecular mechanism of α7 nAChRs' action remains elusive. We previously reported that activation of α7 nAChRs induced a prolonged enhancement of glutamatergic synaptic transmission in a PKA-dependent manner. Here, we investigated any connection between the activation of the α7 nAChR and cAMP signaling in hippocampal neurons. To address this question, we employed a FRET-based biosensor to measure the intracellular cAMP levels directly via live cell imaging. We found that application of the α7 nAChR-selective agonist choline, in the presence of the α7 nAChR positive allosteric modulator PNU-120596, induced a significant change in emission ratio of F535/F470, which indicated an increase in intracellular cAMP levels. This choline-induced increase was abolished by the α7 nAChR antagonist MLA and the calcium chelator BAPTA, suggesting that the cAMP increase depends on the α7 nAChR activation and subsequent intracellular calcium rise. The selective AC1 inhibitor CB-6673567 and siRNA-mediated deletion of AC1 both blocked the choline-induced cAMP increase, suggesting that calcium-dependent AC1 is required for choline's action. Furthermore, α7 nAChR activation stimulated the phosphorylation of synapsin, which serves as a downstream effector to regulate neurotransmitter release. Our findings provide the first direct evidence to link activation of α7 nAChRs to a cAMP rise via AC1, which defines a new signaling pathway employed by α7 nAChRs. Our study sheds light into potential molecular mechanisms of the positive cognitive actions of α7 nAChR agonists and development of therapeutic treatments for cognitive impairments.

Keywords

α7 nAChRs; calcium; AC1; cAMP; synapsin

Corresponding author: Jerrel L Yakel, Neurobiology Laboratory, NIEHS / NIH 111 T.W. Alexander Dr., Durham, NC 27709 yakel@niehs.nih.gov.

The authors declare no competing financial interests.

1. Introduction

The nicotinic ACh receptors (nAChRs) are in the superfamily of cys-loop cationic pentameric channels comprised of six α (2 – 7) and three β (2 – 4) nAChR subunits in the mammalian brain (Nashmi and Lester, 2006). They are activated by endogenous cholinergic inputs and exogenous compounds like nicotine. The α7 nAChR is one of most prevalent nAChR subtypes in the hippocampus (Jones et al., 1999; Albuquerque et al., 2009). Physiological studies have shown that α7 receptors have higher calcium permeability and lower affinity for acetylcholine than other nAChR subtypes (Albuquerque et al., 2009). Besides evoking brief current responses, nAChR agonists also affect neuronal function in a long lasting fashion (Lena and Changeux, 1997; Zhong et al., 2008; Zhong et al., 2013). Activation of α7 nAChRs via rapid stimulation of cholinergic inputs or acetylcholine application induced long-term potentiation (LTP) of synaptic transmission from CA3 to CA1 (Ji et al., 2001; Ge and Dani, 2005; Gu and Yakel, 2011). However how the α7 receptor is enhancing LTP, and furthermore the signaling mechanisms downstream of nAChR activation, remain elusive.

Recently, we found that activation of α7 nAChRs enhanced mossy fiber transmission in a PKA-dependent manner (Cheng and Yakel, 2014). In addition, inhibition of PKA in the dorsal hippocampus abolished nicotine's effect on learning (Gould et al., 2014). It is well accepted that activation of adenylyl cyclases (ACs) can increase glutamate release from hippocampal neurons (Chavez-Noriega and Stevens, 1994; Leenders and Sheng, 2005; Moulder et al., 2008). Moreover, α7 nAChRs were found to be physically associated with AC1 within lipid rafts of airway epithelium (Maouche et al., 2013). AC1 is one of the calcium- and calmodulin-activated ACs and highly expressed in the dendritic arbors of the dentate gyrus and the mossy fiber projections (Nicol et al., 2005; Conti et al., 2007). Based on these facts, we hypothesized that α7 nAChRs exert their long-term actions in part through the mobilization of calcium and activation of calcium-dependent AC1. To test this hypothesis, we directly monitored intracellular cAMP levels through a FRET-based cAMP sensor $^{T}Epac^{VV}$ in real time in individual hippocampal neurons. We found that α7 nAChR activation led to a robust increase in cAMP level, which was blocked by α7 nAChR antagonists, the calcium chelator BAPTA, an AC1 inhibitor, and was reduced by siRNA against AC1. In addition, α7 nAChR activation resulted in the phosphorylation of synapsin. Our data suggest that the α7 nAChR employs the cAMP-PKA signaling pathway to phosphorylate synapsin, thereby mediating its modulation of synaptic transmission and positive actions on cognition. Delineating the downstream signaling pathway after α7 nAChR activation provides potential therapeutic targets, which could work in conjunction with nAChR agonists to treat cognitive disorders.

2. Materials and Methods

2.1 Hippocampal neuronal culture

All animal procedures were conducted in accordance with National Institutes of Health animal welfare guidelines. Wild type C57Bl/6J mice were purchased from Charles River. Postnatal day 0–2 pups of either sex were decapitated, and the hippocampi were removed, treated with papain (Worthington), and serially triturated. The dissociated neurons were

plated onto poly-D-lysine coated glass coverslips. Cells were first cultured in FBS containing Neurobasal-A medium (Life technologies), and then switched to serum-free Neurobasal-A medium after 24 hours.

2.2 Plasmids and siRNAs

We obtained a FRET-based cAMP sensor $^{T}Epac^{VV}$ from Dr. Jalink (University of Amsterdam, Netherlands) (Klarenbeek et al., 2011). The construct was confirmed by sequence analysis. The rat α7 nAChR plasmid was obtained from James Patrick at the Baylor College of Medicine (Houston, TX) (Seguela et al., 1993), and tested in α7 nAChR knockout mice (Gu et al., 2012). GCaMP3 was purchased from Addgene (plasmid no. 22692). Neurons were co-transfected with the cAMP sensor and α7 nAChR plasmids, or the GCaMP3 plasmid, after 3–4 days in culture via Lipofectamine 2000 (Life technologies). Imaging experiments were performed 4–7 days after transfection. Customized On-Target plus siRNA against mouse Adcy1 were purchased from Dharmacon of GE Healthcare. Smart pool siRNA target sequences are: UGGCAAGUUCGAUGAGUUA, GCUCAUGCUGCCGGAAA, GUACAAACAUGUCGAACGA, GGACUUGACAUGAUCGAUA. Non-targeting pool siRNA sequences are: UGGUUUACA-UGCGACUAA, UGGUUUACA-UGUUGUGUGA, UGGUUUACAUGUUUUCUGA, UGGUUU-ACAUGUUUCCUA. For siRNA experiments, siRNA and plasmids were co-transfected using DharmaFECT Duo Transfection reagent (Dharmacon of GE healthcare).

2.3 FRET imaging and data analysis

Hippocampal neurons less than 15 μm in diameter were imaged with a Zeiss LSM 510 META confocal microscope using a 63x, 1.1 NA water immersion objective. Images were collected with Zen2009 software (Carl Zeiss). The sensor was excited at 458 nm by an Argon ion laser, and emitted signals were detected simultaneously through 470–510 nm (F470) and 535–590 nm (F535) band-pass filters. Most FRET experiments were done at 30–60 % power of the 458 nm Argon laser (output at 7.5 mW). The images were captured every 6s automatically. Images were analyzed with Zen2009 and OriginPro 8.5 (OriginLab Corporation). FRET ratio was expressed as ratio of F535 to F470 signals, and calculated for each region of interest (ROI). Mean FRET ratios were averaged from 8–12 ROIs selected randomly from peri-nuclear soma and primary process of each neuron. The mean baseline FRET ratio was obtained via averaging 1 min before the drug application. Choline-induced changes were calculated by averaging the FRET ratios during 9–10th min drug application. The effect of different chemicals was assessed by comparing the mean FRET ratios. Data are plotted as the mean ±SEM. Statistical tests were performed either with unpaired (for group comparison) or paired (for the same cell) Student's t tests.

The experiments were conducted at room temperature in extracellular solution containing (mM): NaCl 140; KCl 3; $MgCl_2$ 2; $CaCl_2$ 2; HEPES 20; glucose 10; pH adjusted to 7.3 with NaOH. To isolate the responses from nAChRs, the imaging experiments were performed in the presence of CNQX and APV (to block glutamate channels), and TTX (to block voltage-gated sodium channels). To amplify the cAMP rise, 50μM IBMX (PDE inhibitor) was added as well. For calcium-free condition, we removed $CaCl_2$ from extracellular solution, and pre-

incubated the neurons with 20 μM BAPTA-AM (Life technology) in Ca-free condition for 30 minutes before imaging. TTX, CNQX, APV, and PNU-120596 were purchased from Tocris. All other compounds were purchased from Sigma unless stated otherwise.

2.4 Immunocytochemistry

Cultured neurons were fixed in 4% paraformaldehyde in phosphate buffer for 15 minutes, permeabilized with 0.25% Triton X-100 for 15 minutes and blocked with 10% normal goat serum for 1 hour. Then neurons were incubated with primary antibody, either rabbit anti-AC1 (1:500, Novus Biologicals, catalog # NBP1-19628) or rabbit anti-p-synapsin Ia/Ib (ser 9) antibody (1:500, Santa Cruz, catalog # sc-135710), at 4°C for overnight, and followed by secondary antibody goat anti-rabbit with DyLight 633 (1:1000, Novus Biologicals, catalog # NBP1-76077) at room temperature for 1 hour. After washing, coverslips were mounted in Vectashield anti-fade mounting medium with Dapi (Vector laboratories). Images were acquired via Zeiss LSM 710 confocal microscope with a 63x/oil immersion objective, and analyzed and processed using MetaMorph (Molecular Devices and Adobe Photoshop (Adobe system). For each condition, we analyzed three coverslips from different neuronal cultures and 8–12 field of views. The phospho-synapsin puncta were selected using integrated morphometric analysis after intensity thresholding. The morphometric parameter for the size of area is 0.1 to 3 μm^2.

3. Results

3.1 The cAMP sensor $^{T}Epac^{VV}$ detects forskolin-induced rise of cAMP in cultured hippocampal neurons

First, we examined the functional properties of the FRET-based cAMP sensor $^{T}Epac^{VV}$ in cultured mouse hippocampal neurons. The sensor contains the cAMP-binding protein Epac1 (**e**xchange **p**roteins **a**ctivated by **c**yclic AMP) and mTurquoise as donor and a double acceptor consisting of a tandem of Venus and ^{cp173}Venus. The increase of cellular cAMP levels leads to a conformational change in Epac1 and a reduction of FRET between donor and acceptor fluorescent proteins. We observed uniform cytosolic distribution of $^{T}Epac^{VV}$ fluorescence in both the soma and processes of hippocampal neurons (Fig. 1A). The sensor-expressing neurons displayed normal morphology, even at high expression levels, without any apparent adverse effects in these neurons. Next, we tested if this sensor displayed a cAMP-dependent change of FRET ratio with forskolin, an activator of most forms of adenylyl cyclases (AC). To maximize the cAMP signal, IBMX (50 μM), a phosphodiesterase (PDE) inhibitor, was added to the bath solution to prevent the breakdown of cAMP and maintain a sustained cAMP elevation. The addition of forskolin (20 μM) increased the fluorescence intensity of mTurquoise, along with the concomitant decrease of Venus fluorescence intensity, in hippocampal neurons (Fig. 1B). Accordingly, the ratio of Venus to mTurquoise fluorescence (F535/F470) demonstrated a robust decrease (Fig. 1A and 1C) in all 6 neurons tested with forskolin (Fig. 1D). The averaged FRET ratio at the 10th minute of forskolin application showed a significant reduction of 19.6 ± 3.6% compared to control (2.4 ± 0.8%, p=0.0008, n=6; Fig. 1E). The forskolin-induced FRET ratio reduction was comparable in magnitude and latency to that seen for this sensor in

stable cell lines (Klarenbeek et al., 2011; Polito et al., 2013). These results suggest that $^{T}Epac^{VV}$ maintains its function as a cAMP sensor in hippocampal neurons.

3.2 Activation of a7 nAChRs increases intracellular cAMP levels in hippocampal neurons

Next, we tested if activation of α7 nAChRs could alter the cAMP levels and thus change the FRET ratio of this sensor. To reduce the variability of endogenous α7 nAChR expression levels in our cultured hippocampal neurons (Zhang et al., 1998; Liu et al., 2001), we routinely co-transfected the α7 nAChR with $^{T}Epac^{VV}$ for our experiments. The expression of α7 nAChRs did not change the expression pattern of $^{T}Epac^{VV}$, and the basal FRET ratio was similar throughout the soma and neuronal processes (Fig. 2A). We bath applied choline (α7 nAChR-selective agonist, 2 mM) together with PNU-120596 (an α7 nAChR positive allosteric modulator [PAM]; 5 μM) to induce substantial and prolonged activation of α7 nAChRs. After 3 to 5 minutes of choline and PNU-120596 application, we observed an initial reduction in the FRET ratio among all selected regions (soma and processes), which reached a maximum around 8–10 minutes after application (Fig. 2C, D). The slowness in response initiation was due to slow bath perfusion, which was necessary to prevent movement during imaging. The averaged FRET ratio at the 10th minute of forskolin application showed a significant reduction of 14.9 ± 1.8% compared to control (4.8 ± 0.5%, p=0.02, n=20; Fig. 2F). Therefore the choline and PNU-120596-induced FRET ratio reduction indicated a significant increase in intracellular cAMP levels. We further analyzed the FRET ratio data by separating FRET signals into two groups: soma and neurite (neuronal processes at least 10 μm away from cell bodies). We found that the basal FRET ratio is very similar between the two groups (soma: 1.29±0.03, and neurites: 1.29±0.16, *t*-test, *p*=0.96), however the neurite group has a larger standard error due to its lower fluorescence intensity (5.3 a.u. versus 32.5 a.u. for the soma). This data suggests that while the cAMP level is similar throughout the neurons, the difference between different compartments could not be differentiated by the current cAMP sensor (with an EC_{50} value of about 14 μM) due to the lower signal-to-noise ratio in the neurites. The treatment of choline and PNU-120596 resulted in a significant FRET ratio change of 13.9±1.5% in the soma group (compared to the control of 2.9±0.7%), and 12.9±1.7% in the neurite group (not statistically different from control of 13.9±1.2%). Though we noticed that the FRET ratio did show a comparable degree of reduction for both the soma and neurite groups, the measurement from neurites is undermined by the low fluorescence intensity and inherent higher noise level. Therefore we could not gain much information from the measurement derived from the neurites.

3.3 Choline-induced cAMP increase requires α7 nAChR activation and subsequent calcium rise

To determine whether the choline and PNU-120596-induced cAMP increase requires activation of α7 nAChRs, we measured the FRET ratio in the presence of MLA (a selective α7 nAChR antagonist). Application of MLA (40 nM) completely blocked the choline and PNU-120596-induced FRET ratio change (2.6 ± 1.9%, n=24, p=0.0006, Fig. 2G-I). Furthermore, choline and PNU-120596 also failed to induce any FRET ratio change in neurons transfected with the cAMP sensor alone (i.e. without the α7 nAChR) at the age of 6 DIV (data not shown), when the endogenous expression of α7 nAChRs could not be

detected both electrophysiologically and biochemically (Colon-Saez and Yakel, 2011). These results suggested that the cAMP increase depends on α7 nAChR activation.

Since the α7 nAChR is highly permeable to calcium, we tested whether the choline and PNU-120596-induced FRET ratio change depended on calcium. First, we confirmed that there was an increase in cytoplasmic calcium levels induced by choline and PNU-120596 using the genetic calcium indicator, GCaMP3. As expected, the fluorescence of GCaMP3 increased sharply upon choline and PNU-120596 application, reaching a peak in 20–30 seconds, and decreased back to baseline within 3 to 5 minutes (Fig. 3A, B). Next, we removed calcium from the extracellular solution and incubated the neurons with BAPTA-AM (20 μM) for 30 minutes before imaging. In this calcium-free condition, choline and PNU-120596 failed to induce any FRET ratio change (3.2 ± 1.3 %, n=16, p=0.0002, Fig. 3C-E). This data indicated that the choline and PNU-120596-induced cAMP increase depends on the α7 nAChR-evoked intracellular calcium rise.

3.4 Choline-induced cAMP increase requires AC1 activation

Based on our observation that activation of the α7 nAChR induced increases in cytoplasmic levels of calcium and cAMP, and that the latter depended on calcium, we hypothesized that the α7 nAChR-induced calcium rise may be activating a calcium-dependent adenylyl cyclase (AC), which in turn led to the production of cAMP. There are two known types of calcium-activated ACs in hippocampal neurons, AC1 and AC8 (Hanoune and Defer, 2001; Conti et al., 2007; Wang and Zhang, 2012). Our previous study showed that the PKA-dependent enhancement of glutamate release was mediated by activation of α7 nAChRs in the hippocampal mossy fiber terminals, which originated from dentate granule cells. AC1 is highly expressed in both dentate granule cell dendrites and mossy fiber axons (Conti et al., 2007). Therefore, we asked if the choline and PNU-120596-induced cAMP rise required the activity of AC1. To test this, we measured the FRET ratio change in the presence of a selective AC1 inhibitor CB-6673567 (50 μM) (Brand et al., 2013). The addition of CB-6673567 alone did not change the basal FRET ratio, suggesting that the basal AC1 activity is low. In the presence of CB-6673567, the choline and PNU-120596-induced FRET ratio change was greatly reduced (3.1 ± 2.5 %, n=14, p=0.002, Fig. 4A-C), suggesting that calcium-dependent AC1 is required for α7 nAChR's action.

Next we asked if the knockdown of AC1 would block choline's action. To test this, we compared the effect of small interfering RNAs (siRNAs) targeted against AC1 and a scrambled siRNA in transfected neurons. To evaluate the efficiency of these siRNAs, we measured the AC1 immunoreactivity from neurons 72 hours after siRNA and EPAC transfection. The EPAC expression was comparable among control neurons, and neurons treated with either scrambled siRNA, or siRNA against AC1 (47.9 ± 5.7 AU, 43.3 ± 4.4 AU and 45.6 ± 2.9 AU respectively, Fig. 4F). On the contrary, the immunoreactivity to AC1 of EPAC-expressing neurons was greatly reduced after treatment of siRNA against AC1 (45.4 ± 3.3 AU, n=87) compared to that of scrambled siRNA (75.2 ± 5.2 AU, n=73, p<0.01) (Fig. 4D, E). This data suggested that siRNA against AC1 successfully reduced the level of AC1. Then, we examined the choline and PNU-120596-induced FRET ratio change in siRNA-treated neurons. Choline and PNU-120596 failed to reduce the FRET ratio in neurons

treated with siRNA targeted against AC1 (Fig. 4H), while they reduced the FRET ratio in non-target scrambled siRNA treated neurons (Fig. 4G). The choline-induced FRET ratio change in non-target scrambled siRNA treated neurons was not significantly different from that of non-treated control neurons (13.9± 2.6%, n=17, p=0.80, Fig. 4I), but in neurons treated with siRNA targeted against AC1, the choline-induced FRET ratio change was significantly smaller than that of control neurons (4.2 ± 1.5 %, n=21, p=0.017, Fig. 4I). These results suggested that AC1 is required for the choline-induced cAMP rise in hippocampal neurons.

3.5 α7 nAChR activation leads to the phosphorylation of synapsin

Lastly to identify possible downstream targets of the α7 nAChR-AC1-PKA cascade, we examined the phosphorylation status of one of the prominent PKA substrates at presynaptic terminals, synapsin (Huttner and Greengard, 1979). To determine if the phosphorylation of synapsin occurred upon activation of α7 nAChRs, we stained the hippocampal neurons with a phospho-specific antibody directed against the PKA phosphorylation site (serine 9) of synapsin I (Hilfiker et al., 2005). At the basal level, synapsin phosphorylation at serine 9 was very sparse and only observed in a small subset of terminals (Figure 5A). Incubation with 20 μM forskolin resulted in the widespread phosphorylation of synapsin as expected. Treatment of choline and PNU-120596 for 4 minutes produced a similar effect to that of forskolin. Quantitative measurements showed a significant increase in the number of puncta containing phosphorylated synapsin in either forskolin or choline and PNU-120596 treated neurons (Figure 5B). The size and fluorescence intensity of the puncta also displayed significant increases for either forskolin or choline and PNU-120596 treated neurons (Figure 5C and 5D). These data suggested that activation of α7 nAChRs leads to the phosphorylation of synapsin at the PKA site.

4. Discussion

cAMP has long been thought of as a gating molecule to control the expression of short-term plasticity and its conversion to long-term plasticity (Kandel, 2012; Kandel et al., 2014). In this study, we investigated its involvement in α7 nAChR-mediated signaling mechanisms with a cAMP biosensor in live cultured mouse hippocampal neurons. We found that activation of α7 nAChRs induced an elevation in intracellular cAMP levels, which depended on the rise of cytoplasmic calcium and activation of the calcium-activated adenylyl cyclase, AC1.

In contrast to biochemical measurements, fluorescence sensors allow us to study the dynamic change in cAMP levels in individual live neurons. We employed the $^{T}Epac^{VV}$ sensor (Klarenbeek et al., 2011) for its brightness, reduced pKa value (less sensitive to pH change), and large dynamic range. Even in the presence of IBMX, we observed low basal cAMP levels in our cultured neurons, indicating little basal AC activity, similar to the report from cortical neurons (Yamashita et al., 1997). In addition, the intracellular cAMP level in neurons can vary depending on cell types, preparations, and developmental stages (Nikolaev et al., 2004; Willoughby and Cooper, 2008; Castro et al., 2010). In contrast to the consistent forskolin-induced cAMP increase, there was more variability in the α7 nAChR-induced increase in cAMP levels; this could stem from differential density of α7 nAChRs, calcium

buffering capacity, and distribution of calcium-dependent AC1 in cultured hippocampal neurons.

Here we have provided several lines of evidence suggesting that the choline and PNU-120596-induced cAMP increase depended on activation of the α7 nAChRs: 1) the cAMP increase was induced by choline, the α7 nAChR-selective agonist, and PNU-120596, the α7 nAChR-selective PAM; 2) the cAMP increase was blocked by a low concentration of MLA (40 nM), an α7 nAChR-selective antagonist; and 3) the cAMP increase was present only in neurons co-transfected with the cAMP sensor and the α7 nAChR subunit. The α7 nAChRs have a high calcium permeability, comparable to that of NMDA receptors (Uteshev, 2012), which confers an ability to transduce a brief ionic current to a long-lasting activation of signaling molecules (Fagen et al., 2003; McKay et al., 2007). Indeed, we observed a prominent calcium rise upon activation of α7 nAChRs via fluorescent imaging using the genetically-encoded calcium sensor GCaMP3. The calcium rise could come from calcium influx through opened α7 nAChRs, as well as the secondary activation of voltage-gated calcium channels, or calcium-induced calcium release from intracellular calcium stores (Sharma and Vijayaraghavan, 2003; Dajas-Bailador and Wonnacott, 2004). When we removed external calcium and chelated internal calcium with BAPTA, activation of α7 nAChRs now failed to increase cAMP levels, suggesting that a subsequent calcium rise following α7 nAChR activation is required for the cAMP increase. This also suggests that there might not be a direct interaction between the α7 nAChR and ACs, but rather that calcium is the intermediate signaling molecule to couple the activation of α7 nAChRs to the cAMP pathway.

Traditionally, the calcium signaling cascade induced by α7 nAChRs is linked to the CaMKII pathway (Sharma et al., 2008), although several studies have linked the activation of α7 nAChRs to cAMP-dependent responses. In the perforant pathway to dentate granule cells, the acute nAChR enhancement of LTP required activation of PKA (Welsby et al., 2009). In cultured hippocampal neurons, nicotine increased the activity of ERK1/2 via α7 nAChR activation in a calcium- and PKA-dependent manner (Dajas-Bailador et al., 2002). In addition, we recently reported that the action of α7 nAChRs at mossy fiber terminals also depended on PKA activity (Cheng and Yakel, 2014). AC1 and AC8 are the only two calcium-dependent ACs in rodent hippocampus. During the early development of the rodent brain, mRNA of AC1 was very high in the cerebral cortex, striatum, thalamus and brainstem, and decreased considerably after third the postnatal week (Matsuoka et al., 1997; Nicol et al., 2005). Conversely, AC8 has very low and limited expression during development and begins to express strongly in mature neurons (Nicol et al., 2005). AC1 plays a crucial role in the refinement of axonal arbors in the somatosensory and visual system in early development stages (Nicol et al., 2006; Nicol et al., 2007; Dhande et al., 2012). AC1 is concentrated in the mossy fiber tract in the mature hippocampus (Conti et al., 2007), and deletion of AC1 led to deficiencies in mossy fiber LTP (Villacres et al., 1998) and impaired spatial memory (Wu et al., 1995). Moreover, calcium-stimulated AC-dependent PKA activation in presynaptic terminals was shown to be primarily driven by AC1, but not AC8, in hippocampus (Conti et al., 2009). Lastly, the α7 nAChR and AC1 were reported to associate physically and functionally in epithelium (Maouche et al., 2013). Here we have shown that either the selective AC1 inhibitor, or knockdown of AC1 with

siRNA, blocked the α7 nAChR-mediated cAMP increase, suggesting that the calcium-dependent AC1 is the key signaling molecule for translating the short calcium rise to cAMP signaling when the α7 nAChRs are activated. If activation of α7 nAChRs, which increases the concentration of cAMP at presynaptic terminals, is accompanied by another depolarization and calcium influx, the strengthening of synaptic transmission would be further enhanced (Gu and Yakel, 2011).

Recently, we found that nAChR activation also converged with the cAMP-PKA signaling pathway to enhance neurotransmission at mossy fiber terminals (Cheng and Yakel, 2014). The cAMP-PKA pathway has long been shown to play a major role in synaptic plasticity at mossy fiber terminals (Huang et al., 1994; Weisskopf et al., 1994; Huang et al., 1995). However, the effectors downstream of this signaling pathway remain elusive. Evidence has shown the PKA-dependent enhancement of synaptic efficacy through the recruitment of synaptic vesicles (SVs) from the reserve pool to the readily releasable pool of vesicles (Trudeau et al., 1996; Kuromi and Kidokoro, 2000; Park et al., 2014). Synapsins, a prominent PKA substrate (Huttner and Greengard, 1979), can regulate neurotransmitter release via mobilization of SVs in the reserve pool (Hilfiker et al., 1999) and alteration of the kinetics of SV fusion (Hilfiker et al., 1998; Humeau et al., 2001; Samigullin et al., 2004; Hilfiker et al., 2005). Additionally, PKA-mediated synapsin I phosphorylation served as a key modulator for calcium-dependent synaptic plasticity (Menegon et al., 2006; Fiumara et al., 2007; Cousin and Evans, 2011). This makes synapsin a suitable candidate to transduce the α7 nAChR-induced calcium and subsequent cAMP rise into the enhancement of glutamate release. Indeed, we found that the activation of α7 nAChRs leads to the widespread increase of phosphorylated synapsin I (via its PKA site), similar to the extent of direct AC activation by forskolin. The enhancement of neurotransmitter release is most likely to involve other PKA substrates besides synapsin. Among them, RIM1α is known to be essential for PKA-dependent LTP in the cerebellum (Lonart et al., 2003).

5. Conclusion

Activation of α7 nAChRs regulates the release of neurotransmitter and synaptic plasticity (Ji et al., 2001; Ge and Dani, 2005; Gu and Yakel, 2011; Cheng and Yakel, 2014), and promotes the maturation of adult-born neurons (Campbell et al., 2010) and glutamate synapse formation (Lozada et al., 2012); these various actions are the result of triggering various signaling cascades. Our results identify a cAMP-dependent pathway as one of the molecular mechanisms employed by the α7 nAChR. Recent studies have shown that targeting α7 nAChRs offers symptomatic improvement of cognitive deficits in Alzheimer's disease, schizophrenia, and Down syndrome (Levin et al., 2006; Thomsen et al., 2010; Deutsch et al., 2013; Deutsch et al., 2014). Our finding provides insight for the development of therapeutic treatments for these and possibly other neuronal disorders. Future studies will determine which presynaptic proteins are the substrates of the α7 nAChR-activated PKA, and how they enhance the release of glutamate.

Acknowledgments

We thank Pattie Lamb and Jeff Tucker for technical support. We appreciate Drs. Georgia Alexander and Shannon Farris for the helpful reading and suggestions on our manuscript. This research was funded by the NIEHS Intramural Research Program/NIH.

Abbreviations

ACh	acetylcholine
cAMP	Cyclic adenosine monophosphate
nAChR	nicotinic acetylcholine receptor
AC	adenylyl cyclase

References

Albuquerque EX, Pereira EF, Alkondon M, Rogers SW. Mammalian nicotinic acetylcholine receptors: from structure to function. Physiol Rev. 2009; 89:73–120. [PubMed: 19126755]

Brand CS, Hocker HJ, Gorfe AA, Cavasotto CN, Dessauer CW. Isoform selectivity of adenylyl cyclase inhibitors: characterization of known and novel compounds. J Pharmacol Exp Ther. 2013; 347:265–275. [PubMed: 24006339]

Campbell NR, Fernandes CC, Halff AW, Berg DK. Endogenous signaling through alpha7-containing nicotinic receptors promotes maturation and integration of adult-born neurons in the hippocampus. J Neurosci. 2010; 30:8734–8744. [PubMed: 20592195]

Castro LR, Gervasi N, Guiot E, Cavellini L, Nikolaev VO, Paupardin-Tritsch D, Vincent P. Type 4 phosphodiesterase plays different integrating roles in different cellular domains in pyramidal cortical neurons. J Neurosci. 2010; 30:6143–6151. [PubMed: 20427672]

Chavez-Noriega LE, Stevens CF. Increased transmitter release at excitatory synapses produced by direct activation of adenylate cyclase in rat hippocampal slices. J Neurosci. 1994; 14:310–317. [PubMed: 7506766]

Cheng Q, Yakel JL. Presynaptic alpha7 nicotinic acetylcholine receptors enhance hippocampal mossy fiber glutamatergic transmission via PKA activation. J Neurosci. 2014; 34:124–133. [PubMed: 24381273]

Colon-Saez JO, Yakel JL. The alpha7 nicotinic acetylcholine receptor function in hippocampal neurons is regulated by the lipid composition of the plasma membrane. J Physiol. 2011; 589:3163–3174. [PubMed: 21540349]

Conti AC, Maas JW Jr, Moulder KL, Jiang X, Dave BA, Mennerick S, Muglia LJ. Adenylyl cyclases 1 and 8 initiate a presynaptic homeostatic response to ethanol treatment. PLoS One. 2009; 4:e5697. [PubMed: 19479030]

Conti AC, Maas JW Jr, Muglia LM, Dave BA, Vogt SK, Tran TT, Rayhel EJ, Muglia LJ. Distinct regional and subcellular localization of adenylyl cyclases type 1 and 8 in mouse brain. Neuroscience. 2007; 146:713–729. [PubMed: 17335981]

Cousin MA, Evans GJ. Activation of silent and weak synapses by cAMP-dependent protein kinase in cultured cerebellar granule neurons. J Physiol. 2011; 589:1943–1955. [PubMed: 21486806]

Dajas-Bailador F, Wonnacott S. Nicotinic acetylcholine receptors and the regulation of neuronal signalling. Trends Pharmacol Sci. 2004; 25:317–324. [PubMed: 15165747]

Dajas-Bailador FA, Soliakov L, Wonnacott S. Nicotine activates the extracellular signal-regulated kinase 1/2 via the alpha7 nicotinic acetylcholine receptor and protein kinase A, in SH-SY5Y cells and hippocampal neurones. J Neurochem. 2002; 80:520–530. [PubMed: 11905997]

Deutsch SI, Burket JA, Benson AD. Targeting the alpha nicotinic acetylcholine receptor to prevent progressive dementia and improve cognition in adults with Down's syndrome. Prog Neuropsychopharmacol Biol Psychiatry. 2014; 54C:131–139. [PubMed: 24865150]

Deutsch SI, Schwartz BL, Schooler NR, Brown CH, Rosse RB, Rosse SM. Targeting alpha-7 nicotinic neurotransmission in schizophrenia: a novel agonist strategy. Schizophr Res. 2013; 148:138–144. [PubMed: 23768813]

Dhande OS, Bhatt S, Anishchenko A, Elstrott J, Iwasato T, Swindell EC, Xu HP, Jamrich M, Itohara S, Feller MB, Crair MC. Role of adenylate cyclase 1 in retinofugal map development. J Comp Neurol. 2012; 520:1562–1583. [PubMed: 22102330]

Fagen ZM, Mansvelder HD, Keath JR, McGehee DS. Short- and long-term modulation of synaptic inputs to brain reward areas by nicotine. Ann N Y Acad Sci. 2003; 1003:185–195. [PubMed: 14684446]

Fiumara F, Milanese C, Corradi A, Giovedi S, Leitinger G, Menegon A, Montarolo PG, Benfenati F, Ghirardi M. Phosphorylation of synapsin domain A is required for post-tetanic potentiation. J Cell Sci. 2007; 120:3228–3237. [PubMed: 17726061]

Ge S, Dani JA. Nicotinic acetylcholine receptors at glutamate synapses facilitate long-term depression or potentiation. J Neurosci. 2005; 25:6084–6091. [PubMed: 15987938]

Gould TJ, Wilkinson DS, Yildirim E, Poole RL, Leach PT, Simmons SJ. Nicotine shifts the temporal activation of hippocampal protein kinase A and extracellular signal-regulated kinase 1/2 to enhance long-term, but not short-term, hippocampus-dependent memory. Neurobiol Learn Mem. 2014; 109:151–159. [PubMed: 24457151]

Gu Z, Yakel JL. Timing-dependent septal cholinergic induction of dynamic hippocampal synaptic plasticity. Neuron. 2011; 71:155–165. [PubMed: 21745645]

Gu Z, Lamb PW, Yakel JL. Cholinergic coordination of presynaptic and postsynaptic activity induces timing-dependent hippocampal synaptic plasticity. J Neurosci. 2012; 32:12337–12348. [PubMed: 22956824]

Hanoune J, Defer N. Regulation and role of adenylyl cyclase isoforms. Annu Rev Pharmacol Toxicol. 2001; 41:145–174. [PubMed: 11264454]

Hilfiker S, Schweizer FE, Kao HT, Czernik AJ, Greengard P, Augustine GJ. Two sites of action for synapsin domain E in regulating neurotransmitter release. Nat Neurosci. 1998; 1:29–35. [PubMed: 10195105]

Hilfiker S, Pieribone VA, Czernik AJ, Kao HT, Augustine GJ, Greengard P. Synapsins as regulators of neurotransmitter release. Philos Trans R Soc Lond B Biol Sci. 1999; 354:269–279. [PubMed: 10212475]

Hilfiker S, Benfenati F, Doussau F, Nairn AC, Czernik AJ, Augustine GJ, Greengard P. Structural domains involved in the regulation of transmitter release by synapsins. J Neurosci. 2005; 25:2658–2669. [PubMed: 15758176]

Huang YY, Li XC, Kandel ER. cAMP contributes to mossy fiber LTP by initiating both a covalently mediated early phase and macromolecular synthesis-dependent late phase. Cell. 1994; 79:69–79. [PubMed: 7923379]

Huang YY, Kandel ER, Varshavsky L, Brandon EP, Qi M, Idzerda RL, McKnight GS, Bourtchouladze R. A genetic test of the effects of mutations in PKA on mossy fiber LTP and its relation to spatial and contextual learning. Cell. 1995; 83:1211–1222. [PubMed: 8548807]

Humeau Y, Doussau F, Vitiello F, Greengard P, Benfenati F, Poulain B. Synapsin controls both reserve and releasable synaptic vesicle pools during neuronal activity and short-term plasticity in Aplysia. J Neurosci. 2001; 21:4195–4206. [PubMed: 11404405]

Huttner WB, Greengard P. Multiple phosphorylation sites in protein I and their differential regulation by cyclic AMP and calcium. Proc Natl Acad Sci U S A. 1979; 76:5402–5406. [PubMed: 228290]

Ji D, Lape R, Dani JA. Timing and location of nicotinic activity enhances or depresses hippocampal synaptic plasticity. Neuron. 2001; 31:131–141. [PubMed: 11498056]

Jones S, Sudweeks S, Yakel JL. Nicotinic receptors in the brain: correlating physiology with function. Trends Neurosci. 1999; 22:555–561. [PubMed: 10542436]

Kandel ER. The molecular biology of memory: cAMP, PKA, CRE, CREB-1, CREB-2, and CPEB. Mol Brain. 2012; 5:14. [PubMed: 22583753]

Kandel ER, Dudai Y, Mayford MR. The molecular and systems biology of memory. Cell. 2014; 157:163–186. [PubMed: 24679534]

Klarenbeek JB, Goedhart J, Hink MA, Gadella TW, Jalink K. A mTurquoise-based cAMP sensor for both FLIM and ratiometric read-out has improved dynamic range. PLoS One. 2011; 6:e19170. [PubMed: 21559477]

Kuromi H, Kidokoro Y. Tetanic stimulation recruits vesicles from reserve pool via a cAMP-mediated process in Drosophila synapses. Neuron. 2000; 27:133–143. [PubMed: 10939337]

Leenders AG, Sheng ZH. Modulation of neurotransmitter release by the second messenger-activated protein kinases: implications for presynaptic plasticity. Pharmacol Ther. 2005; 105:69–84. [PubMed: 15626456]

Lena C, Changeux JP. Role of Ca2+ ions in nicotinic facilitation of GABA release in mouse thalamus. J Neurosci. 1997; 17:576–585. [PubMed: 8987780]

Levin ED, McClernon FJ, Rezvani AH. Nicotinic effects on cognitive function: behavioral characterization, pharmacological specification, and anatomic localization. Psychopharmacology (Berl). 2006; 184:523–539. [PubMed: 16220335]

Liu Y, Ford B, Mann MA, Fischbach GD. Neuregulins increase alpha7 nicotinic acetylcholine receptors and enhance excitatory synaptic transmission in GABAergic interneurons of the hippocampus. J Neurosci. 2001; 21:5660–5669. [PubMed: 11466437]

Lonart G, Schoch S, Kaeser PS, Larkin CJ, Sudhof TC, Linden DJ. Phosphorylation of RIM1alpha by PKA triggers presynaptic long-term potentiation at cerebellar parallel fiber synapses. Cell. 2003; 115:49–60. [PubMed: 14532002]

Lozada AF, Wang X, Gounko NV, Massey KA, Duan J, Liu Z, Berg DK. Glutamatergic synapse formation is promoted by alpha7-containing nicotinic acetylcholine receptors. J Neurosci. 2012; 32:7651–7661. [PubMed: 22649244]

Maouche K, Medjber K, Zahm JM, Delavoie F, Terryn C, Coraux C, Pons S, Cloez-Tayarani I, Maskos U, Birembaut P, Tournier JM. Contribution of alpha7 nicotinic receptor to airway epithelium dysfunction under nicotine exposure. Proc Natl Acad Sci U S A. 2013; 110:4099–4104. [PubMed: 23431157]

Matsuoka I, Suzuki Y, Defer N, Nakanishi H, Hanoune J. Differential expression of type I, II, and V adenylyl cyclase gene in the postnatal developing rat brain. J Neurochem. 1997; 68:498–506. [PubMed: 9003034]

McKay BE, Placzek AN, Dani JA. Regulation of synaptic transmission and plasticity by neuronal nicotinic acetylcholine receptors. Biochem Pharmacol. 2007; 74:1120–1133. [PubMed: 17689497]

Menegon A, Bonanomi D, Albertinazzi C, Lotti F, Ferrari G, Kao HT, Benfenati F, Baldelli P, Valtorta F. Protein kinase A-mediated synapsin I phosphorylation is a central modulator of Ca2+-dependent synaptic activity. J Neurosci. 2006; 26:11670–11681. [PubMed: 17093089]

Moulder KL, Jiang X, Chang C, Taylor AA, Benz AM, Conti AC, Muglia LJ, Mennerick S. A specific role for Ca2+-dependent adenylyl cyclases in recovery from adaptive presynaptic silencing. J Neurosci. 2008; 28:5159–5168. [PubMed: 18480272]

Nashmi R, Lester HA. CNS localization of neuronal nicotinic receptors. J Mol Neurosci. 2006; 30:181–184. [PubMed: 17192671]

Nicol X, Muzerelle A, Bachy I, Ravary A, Gaspar P. Spatiotemporal localization of the calcium-stimulated adenylate cyclases, AC1 and AC8, during mouse brain development. J Comp Neurol. 2005; 486:281–294. [PubMed: 15844169]

Nicol X, Muzerelle A, Rio JP, Metin C, Gaspar P. Requirement of adenylate cyclase 1 for the ephrin-A5-dependent retraction of exuberant retinal axons. J Neurosci. 2006; 26:862–872. [PubMed: 16421306]

Nicol X, Voyatzis S, Muzerelle A, Narboux-Neme N, Sudhof TC, Miles R, Gaspar P. cAMP oscillations and retinal activity are permissive for ephrin signaling during the establishment of the retinotopic map. Nat Neurosci. 2007; 10:340–347. [PubMed: 17259982]

Nikolaev VO, Bunemann M, Hein L, Hannawacker A, Lohse MJ. Novel single chain cAMP sensors for receptor-induced signal propagation. J Biol Chem. 2004; 279:37215–37218. [PubMed: 15231839]

Park AJ, Havekes R, Choi JH, Luczak V, Nie T, Huang T, Abel T. A presynaptic role for PKA in synaptic tagging and memory. Neurobiol Learn Mem. 2014; 114:101–112. [PubMed: 24882624]

Polito M, Klarenbeek J, Jalink K, Paupardin-Tritsch D, Vincent P, Castro LR. The NO/cGMP pathway inhibits transient cAMP signals through the activation of PDE2 in striatal neurons. Front Cell Neurosci. 2013; 7:211. [PubMed: 24302895]

Samigullin D, Bill CA, Coleman WL, Bykhovskaia M. Regulation of transmitter release by synapsin II in mouse motor terminals. J Physiol. 2004; 561:149–158. [PubMed: 15388780]

Seguela P, Wadiche J, Dineley-Miller K, Dani JA, Patrick JW. Molecular cloning, functional properties, and distribution of rat brain alpha 7: a nicotinic cation channel highly permeable to calcium. J Neurosci. 1993; 13:596–604. [PubMed: 7678857]

Sharma G, Vijayaraghavan S. Modulation of presynaptic store calcium induces release of glutamate and postsynaptic firing. Neuron. 2003; 38:929–939. [PubMed: 12818178]

Sharma G, Grybko M, Vijayaraghavan S. Action potential-independent and nicotinic receptor-mediated concerted release of multiple quanta at hippocampal CA3-mossy fiber synapses. J Neurosci. 2008; 28:2563–2575. [PubMed: 18322100]

Thomsen MS, Hansen HH, Timmerman DB, Mikkelsen JD. Cognitive improvement by activation of alpha7 nicotinic acetylcholine receptors: from animal models to human pathophysiology. Curr Pharm Des. 2010; 16:323–343. [PubMed: 20109142]

Trudeau LE, Emery DG, Haydon PG. Direct modulation of the secretory machinery underlies PKA-dependent synaptic facilitation in hippocampal neurons. Neuron. 1996; 17:789–797. [PubMed: 8893035]

Uteshev VV. alpha7 nicotinic ACh receptors as a ligand-gated source of Ca(2+) ions: the search for a Ca(2+) optimum. Adv Exp Med Biol. 2012; 740:603–638. [PubMed: 22453962]

Villacres EC, Wong ST, Chavkin C, Storm DR. Type I adenylyl cyclase mutant mice have impaired mossy fiber long-term potentiation. J Neurosci. 1998; 18:3186–3194. [PubMed: 9547227]

Wang H, Zhang M. The role of Ca(2)(+)-stimulated adenylyl cyclases in bidirectional synaptic plasticity and brain function. Rev Neurosci. 2012; 23:67–78. [PubMed: 22718613]

Weisskopf MG, Castillo PE, Zalutsky RA, Nicoll RA. Mediation of hippocampal mossy fiber long-term potentiation by cyclic AMP. Science. 1994; 265:1878–1882. [PubMed: 7916482]

Welsby PJ, Rowan MJ, Anwyl R. Intracellular mechanisms underlying the nicotinic enhancement of LTP in the rat dentate gyrus. Eur J Neurosci. 2009; 29:65–75. [PubMed: 19077124]

Willoughby D, Cooper DM. Live-cell imaging of cAMP dynamics. Nat Methods. 2008; 5:29–36. [PubMed: 18165805]

Wu ZL, Thomas SA, Villacres EC, Xia Z, Simmons ML, Chavkin C, Palmiter RD, Storm DR. Altered behavior and long-term potentiation in type I adenylyl cyclase mutant mice. Proc Natl Acad Sci U S A. 1995; 92:220–224. [PubMed: 7816821]

Yamashita N, Yamauchi M, Baba J, Sawa A. Phosphodiesterase type 4 that regulates cAMP level in cortical neurons shows high sensitivity to rolipram. Eur J Pharmacol. 1997; 337:95–102. [PubMed: 9389386]

Zhang X, Liu C, Miao H, Gong ZH, Nordberg A. Postnatal changes of nicotinic acetylcholine receptor alpha 2, alpha 3, alpha 4, alpha 7 and beta 2 subunits genes expression in rat brain. Int J Dev Neurosci. 1998; 16:507–518. [PubMed: 9881299]

Zhong C, Talmage DA, Role LW. Nicotine elicits prolonged calcium signaling along ventral hippocampal axons. PLoS One. 2013; 8:e82719. [PubMed: 24349346]

Zhong C, Du C, Hancock M, Mertz M, Talmage DA, Role LW. Presynaptic type III neuregulin 1 is required for sustained enhancement of hippocampal transmission by nicotine and for axonal targeting of alpha7 nicotinic acetylcholine receptors. J Neurosci. 2008; 28:9111–9116. [PubMed: 18784291]

Highlights

Activation of α7 nAChRs increases intracellular cAMP levels.

The rise of cAMP is dependent on calcium and AC1.

Activation of α7 nAChRs increases the phosphorylation of synapsin I at its PKA site.

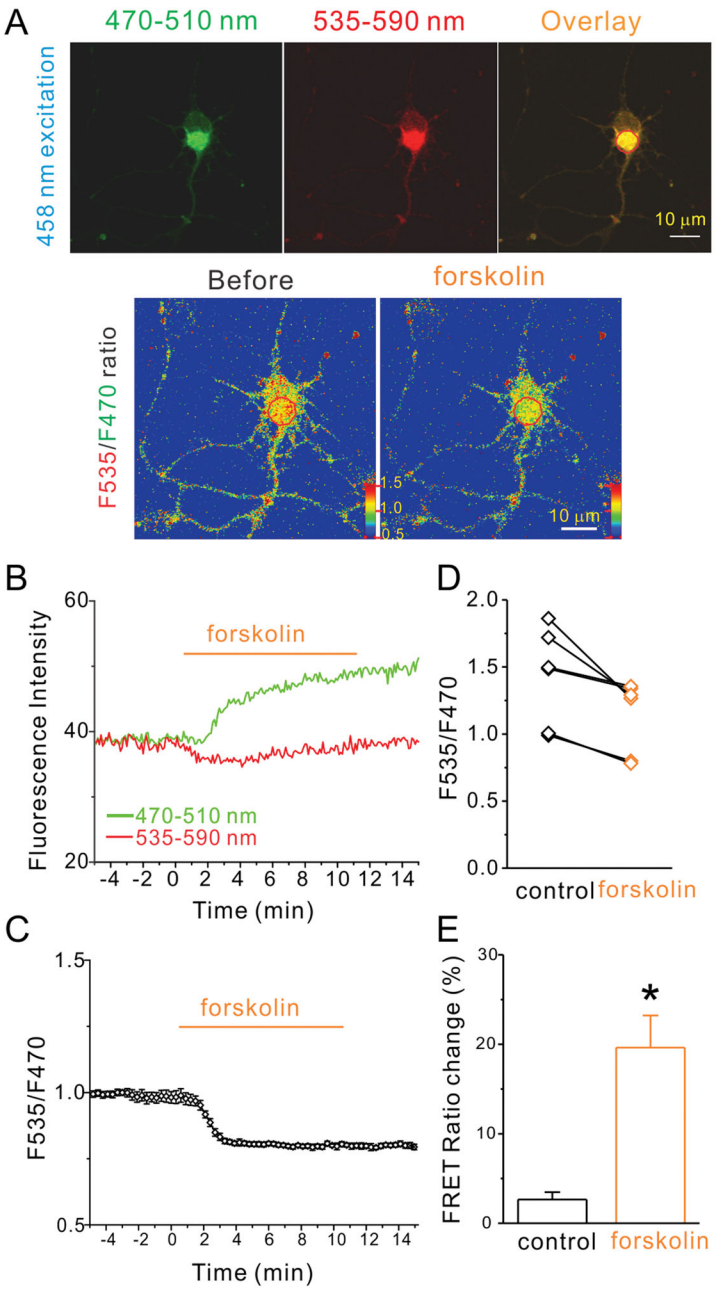

Figure 1.

cAMP sensor maintains its function in cultured hippocampal neurons. (A) Fluorescent images of a representative hippocampal neuron expressing the cAMP sensor $^{T}Epac^{VV}$ excited with 458 nm laser and viewed with 470–510 nm emission spectrum (F470, left upper panel), or 535–590 nm emission spectrum (F535, middle upper panel), and overlay (right upper panel). The lower panel displayed F535/F470 ratio images before (left) and during forskolin application (right) at 10 minute time point. (B) The fluorescence intensity of red circle outlined in the overlay panel of (A) in F470 (green) and F535 (red) spectrums were plotted against time of the bath application of forskolin (20 μM). (C) The FRET ratio (F535/

F470 spectrum) was plotted against the time of bath application of forskolin (20 μM). (D) FRET ratios of 6 tested neurons were plotted against listed conditions. (E) The histogram shows forskolin-induced net decrease of normalized FRET ratio in listed conditions. Data shown are mean ± SEM; statistical significance was determined by Student's *t*-test (* denotes $p<0.05$).

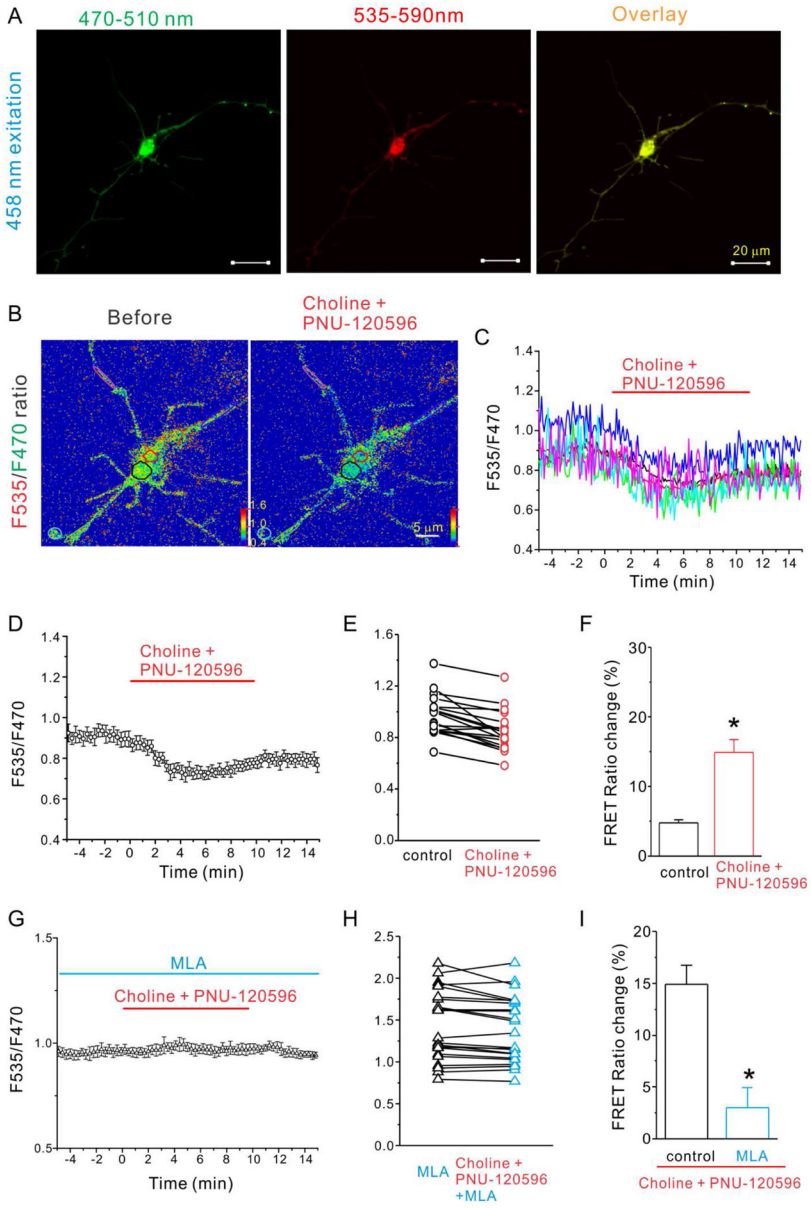

Figure 2.

Choline and PNU-120596 decreased FRET ratio in hippocampal neurons expressing cAMP sensor and α7 nAChRs is dependent on activation of α7 nAChRs. A) Fluorescent images of a representative hippocampal neuron expressing the cAMP sensor $^{T}Epac^{VV}$ and α7 nAChRs excited with 458 nm laser and viewed with 470–510 nm emission spectrum (F470, left), or 535–590 nm emission spectrum (F535, middle), and overlay (right) (scale bar= 20 μm). (B) F535/F470 ratio images before (left) and during choline and PNU-120596 (right) application at 10 minute time point with color coded ROIs. FRET ratios of individual ROIs (C) and the averaged FRET ratio (D) were plotted against the time of bath application of choline (2 mM) and PNU-120596 (5 μM) (from 0 to 10 minutes). The red line indicates the duration of choline and PNU-120596 perfusion. (E) and (H) FRET ratios of tested neurons were plotted against listed conditions. (F) and (I) The histogram shows choline and PNU-120596-induced

net decrease of normalized FRET ratio in listed conditions. (G) The averaged FRET ratio of a representative neuron was plotted against the time before, during and after application of choline (2 mM) and PNU-120596 (5 μM) in the presence of MLA (40 nM) Data shown are mean ± SEM; statistical significance was determined by Student's *t*-test (* denotes $p<0.05$).

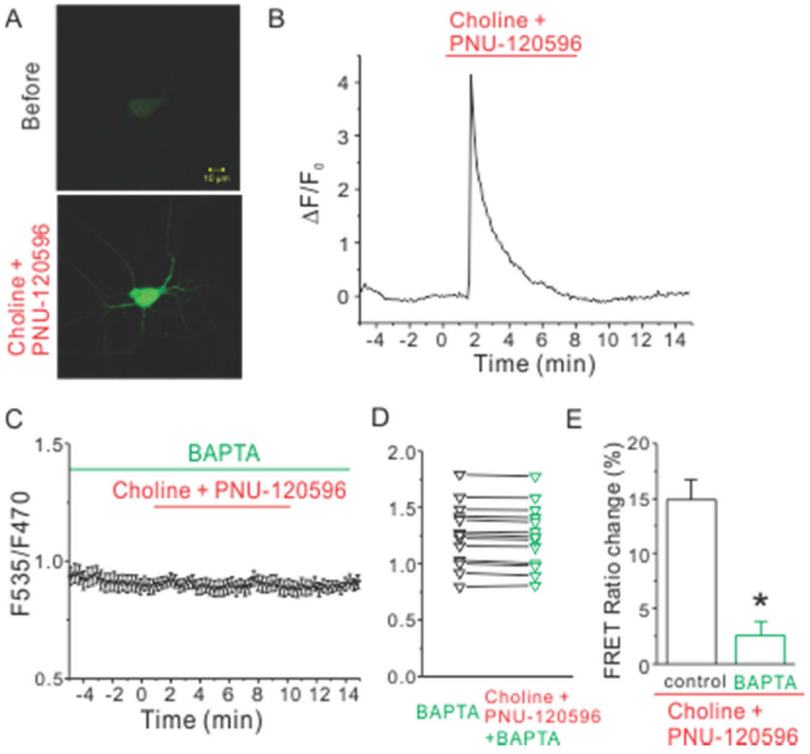

Figure 3.

Choline and PNU-120596 induced a robust intracellular calcium rise which was required for choline and PNU-120596-induced decrease of FRET ratio. (A) Fluorescent images of a representative hippocampal neuron expressing GCaMP3 were shown before (top) and during the application of choline and PNU-120596 (bottom). (B) Time course of fluorescence intensity of GCaMP3 revealed calcium rise evoked by application of choline and PNU-120596. (C) The averaged FRET ratio of a representative neuron transfected with the cAMP sensor $^{T}Epac^{VV}$ and α7 nAChRs was plotted against the time before, during and after application of choline (2 mM) and PNU-120596 (5 μM) in calcium-free conditions. (D) FRET ratios of individual tested neurons were plotted against indicated conditions. (E) The histogram shows choline and PNU-120596-induced net decrease of normalized FRET ratio in listed conditions. * denotes $p<0.05$.

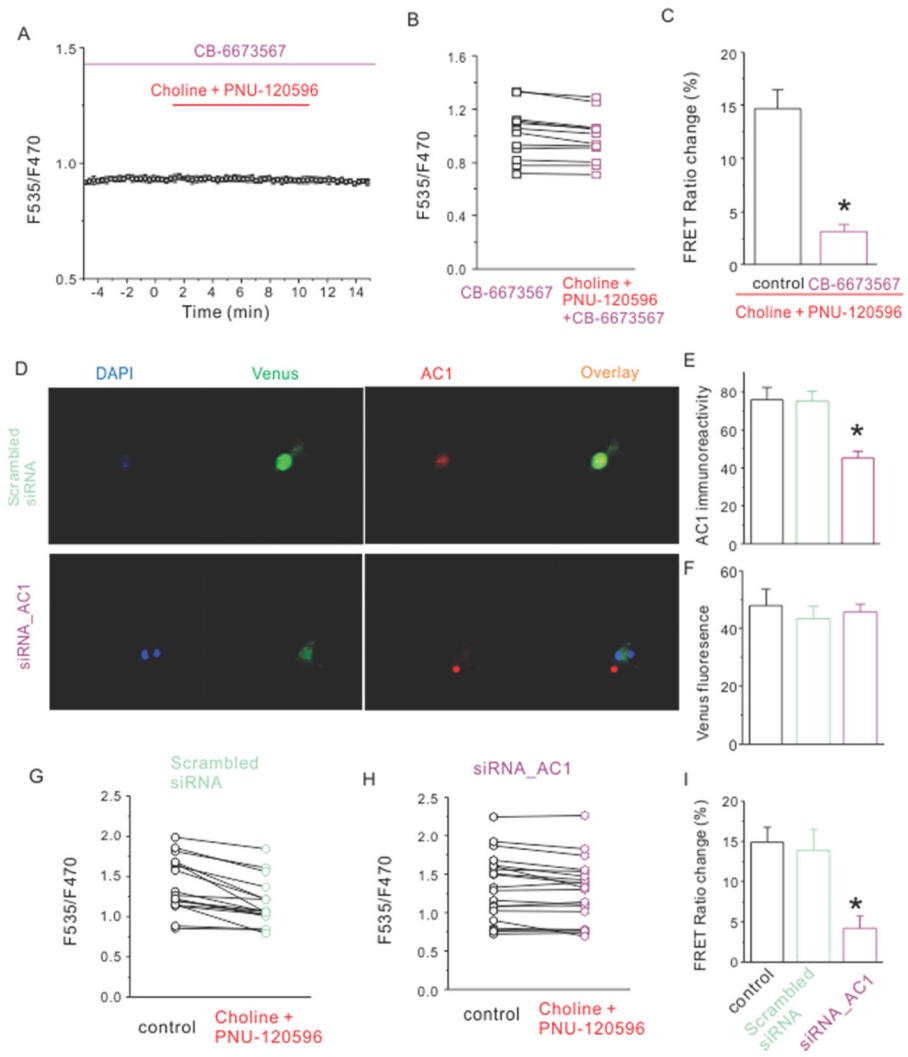

Figure 4.

Either AC1 inhibitor or knockdown of AC1 with siRNA reduced choline and PNU-120596-induced decrease of FRET ratio. (A) The averaged FRET ratio of a representative neuron was plotted against the time before, during and after application of choline (2 mM) and PNU-120596 (5 μM) in the presence of CB-6673567(50 μM). (B) FRET ratios of individual tested neurons were plotted against indicated conditions. (C) The histogram shows choline and PNU-120596-induced net decrease of normalized FRET ratio in listed conditions. (D) Images of neurons transfected with EPAC and α7 nAChRs treated with either scrambled siRNA (upper panel) or siRNA against AC1 (lower panel) were shown with DAPI staining (blue), EPAC fluorescence (green) and immunostaining against AC1 (red). Immunoreactivity against AC1 (E) but not fluorescence intensity of Venus (F) was decreased for neurons treated with siRNA_AC1. The FRET ratios of individual tested neurons were plotted for scrambled siRNA (G) and siRNA against AC1 (H). (I) The histogram shows choline and PNU-120596-induced net decrease of normalized FRET ratio in listed conditions. Data shown are mean ± SEM; statistical significance was determined by Student's *t*-test (* denotes $p<0.05$).

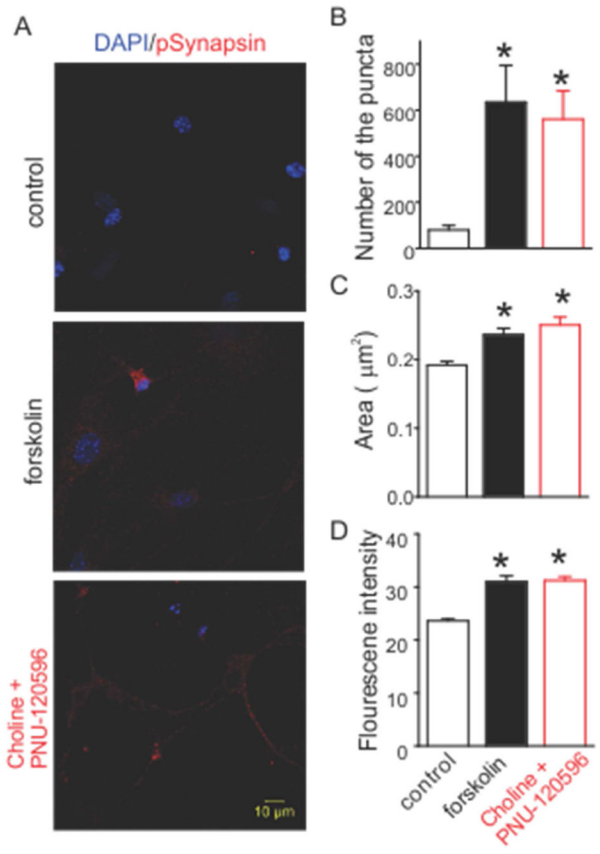

Figure 5.

Activation of α7 nAChR induces the phorphorylation of synapsin at PKA site. (A) Hippocampal neurons were stained against phospho-synapsin I (red) and DAPI (blue). Stimulation with either forskolin (center) or choline and PNU-120596 (right) caused a big increase of immunofluorescence compared to control (left). (B)-(D) Histograms show the changes of the size, fluorescence intensity, and number of phospho-synapsin puncta. Data shown are mean ± SEM; statistical significance was determined by Student's *t*-test (* denotes $p<0.05$).